



# ROISegNet: Anatomy-Aware Deep Learning Framework for Accurate Breast ROI Segmentation in Thermographic Imaging

Preethi Veerlapalli<sup>1\*</sup>, Dr. Sushama Rani Dutta<sup>2</sup>

<sup>1</sup>Research Scholar, Department of Computer Science and Engineering, Koneru Lakshmaiah Education Foundation, Hyderabad-500075, Telangana, India, Email: [preethireddyveerlapalli@gmail.com](mailto:preethireddyveerlapalli@gmail.com), Orcid id: 0000-0003-0468-9717

<sup>2</sup>Department of Computer Science and Engineering, Koneru Lakshmaiah Education Foundation, Hyderabad-500075, Telangana, India. Email: [Sushamarani.dutta@klh.edu.in](mailto:Sushamarani.dutta@klh.edu.in), Orcid id: 0000-0001-7302-0801

\*Corresponding Author

## Abstract

Breast thermography (BT) is a new imaging modality that is a safe, non-invasive method with potential usefulness of early breast abnormalities detection. But the clinical value is restricted by the challenge of reproducibly determining anatomic relevant region of interests (ROIs) under differing thermal conditions, as well as background distractions. This problem indicates the space of automated and strong ROI segmentation techniques. In this work, we propose a semantic segmentation framework based on deep learning specifically for breast thermogram analysis called ROISegNet. Our architecture consists of a hierarchical atrous convolution-based encoder for multi-scale feature extraction, improved atrous spatial pyramid pooling (ASPP) module for context information capturing and a novel anatomy guided ROI localisation strategy ISBROI to reduce irrelevant background pixels and localise breast boundaries. Using the same experimental protocol, the model is evaluated on the publicly accessible DMR-IR dataset and compared with previously established architectures such as VGG19, ResNet50, InceptionV3, and other atrous convolution-based approaches. Experimental results showed that ROISegNet gives promising, consistent, and stable performances with the average accuracy of ~97%, average mean IoU (93–94%), precision, and less Dice loss. These results suggest bounds preservation efficacy and alignment in space. Lastly, statistical validation across numerous experimental runs validates the stability and reproducibility of the proposed framework. We conclude that ROISegNet allows for semi-automatic accurately, anatomically consistently segmentation of breast ROIs, making it a promising preprocessing component in computer-aided analysis systems for thermography. This approach could allow more reliable non-invasive breast screening once further optimisation and validation of the methodology is complete, thereby facilitating early clinical diagnosis.

*Keywords: Breast Thermography, ROI Segmentation, Deep Learning, Atrous Convolution, ASPP, Medical Image Segmentation, ISBROI, Computer-Aided Diagnosis*

This is an open access article under CC BY 4.0, allowing unrestricted use with proper attribution, a license link, and indication of any changes made.

## 1. Introduction

Breast cancer continues to be one of the most important causes of death from cancer among women globally, and early detection is crucial for improving survival. Conventional mammography, ultrasound, and biopsy are frequently used for diagnosis; nonetheless, the aforementioned strategies have disadvantages such as risk of exposure to ionising radiation, a modest sensitivity in dense breast tissues, as well as discomfort for the patient [21], [29]. Consequently, non-invasive imaging techniques have been of increasing interest over the last few years.

Breast thermography, which is based on detection of temperature changes caused by the abnormal physiological functioning [2], [36], has been witnessed a rising interest as the novel modality for early-stage diagnosis. In contrast to conventional imaging, thermography is 100% non-invasive and without radioactivity

and therefore can be used for repeated screening [9], [35]. Many studies showed that thermal imaging with machine learning methods could be a new way for breast cancer detection diagnosis. [1], [4]. Furthermore, hybrid thermal data with clinical and demographic data set have shown improved diagnostic value [3], [6].

However, there are significant challenges to thermographic image analysis. Poor spatial resolution, interference from noises, and overlapping surrounding anatomical areas (such as the neck and shoulders) exacerbate correct interpretation [9], [34]. Perhaps one of the biggest challenges is the reliable detection of breast region of interest (ROI) [38], and this detection will affect inaccuracy of classification then diagnosis as it is presented directly after the pre-processing step. Conventional threshold or needlepoint segmentation methods typically lack the capacity to generalise to a wide variance of thermal patterns, such as [31], [40].

Due to this limitations, comprehensive exploration of machine learning (ML) and deep learning (DL) techniques has been carried out. Thermographic data has been successfully studied with ML- based approaches, for example Support Vector Machines and Random Forest classifiers [7], [12]. Yet, these methodologies are largely dependent on manual feature engineering, restricting their versatility towards complicated image patterns [8], [23]. Convolutional Neural Networks (CNNs) have been considered state-of-the-art and outperformed traditional methods by improving the extraction of hierarchical features from medical images automatically [5], [39].

Over the last several years, the development of deep learning (DL) methods has made it possible to build stronger computer-aided diagnostic systems for the detection of breast cancer in a variety of imaging modalities [18], [26]. In addition, thermal images segmentation and classification methods based on deep learning have also been investigated [30], [33]. Yet, current methods suffer from poor ROI localizability and boundaries in low-contrast thermographic conditions [14], [16].

Moreover, the majority of the current techniques do not impose anatomical limitations on the APP segments, which leads to inappropriate inclusion of out-of-breast tissues. It has experimented with Cascade CNN models and optimisation-based segmentation methods [11], [32] which nonetheless are constrained by their failure to produce consistent segmentation of an anatomically well-defined ROI.

The development of deep learning networks such as initial backpropagation networks [42], through advanced convolutional networks to recognition and localisation [43], [44], [45], and other architectures has made possible far more potent image analysis than was previously feasible. Moreover, techniques [48], multi-scale feature learning [51], [52] and optimisation strategies [50] have been added to improve segmentation performance. Such developments form a strong foundation towards the improved thermographic segmentation architectures.

Inspired by these issues, this work introduces ROIsegNet, a deep learning framework for accurate and anatomically consistent breast ROI segmentation from thermographic images. A multi-scale feature extraction, contextual modelling and an anatomy aware localisation strategy is proposed to ensure reliable and robust segmentations.

## 2. Related Work

### 2.1 Thermography-Based Breast Cancer Detection

Thermography (also known as infrared imaging or thermal imaging) has been studied extensively as a non-invasive method for breast cancer detection, since metabolic and vascular alterations can be detected as temperature variations [36]. Initial works investigated the application of thermal imaging and supervised machine learning for classification and diagnosis [2]. In this respect, hybrid methods combining thermal features with sophisticated feature selection methods based on techniques such as curvelet transforms, and optimisation methods have been underlined to enhance the accuracy of diagnosis [1], [4].

Recently, integration of clinical data and thermal imaging has been used to improve the prediction performances. Some multi-input deep learning approach using (thermal and patient-specific information) have improve the reliability of the diagnosis [3], [6]. Mobile and economical thermography technology has also been suggested for mass screening and remote follow-up [27].

Several extensive reviews have focused on the increasing importance of thermography for breast cancer detection and the potential use of it as an adjunct to standard imaging modalities [9], [33], [34]. Nonetheless, these studies also demonstrate the importance of strong pre-processing and segmentation methods towards increasing the accuracy of the analysis.

## **2.2 Machine Learning and Deep Learning Approaches**

Various machine learning techniques are widely used for classification and detection problems in breast thermography. Classic models such as Decision Trees, Support Vector Machines, and Random Forest classifiers have performed well to some extent to classify abnormal thermal patterns [7], [12]. Detection accuracy has been further enhanced by ensemble and hybrid learning solutions that combine several feature extraction and classification methods [23].

Nevertheless, ML-based methods are constrained by both handcrafted characteristics and difficulty extension to extensive datasets [8]. To address these limitations, deep learning methods, specially CNNs have integrated automatic feature extraction and hierarchical representation learning [5], [39].

Various DL based frameworks have been suggested for breast cancer detection from different imaging techniques, such as thermography, ultrasound, and tomosynthesis [18], [20], [26]. These models outperformed conventional methods in classification and segmentation tasks. Furthermore, hybrid schemes of DL and optimisation based methods have also been used to improve the segmentation performance [11].

There have also been advanced segmentation models such as DeepBatch, other CNN based architectures applied on real world medical imaging tasks offering more interpretability and performance [13], [24]. Similarly, domain-specific approaches utilizing expert knowledge has been successful in enhancing diagnostic outcomes [20].

## **2.3 ROI Segmentation Challenges in Thermography**

Thermographic image analysis continues to face a major issue with accurately segmentation of the breast ROI. Accurate segmentation is challenging due to differences in thermal patterns, variable low contrast, and overlap or interference from surrounding anatomical regions [14], [16]. Traditional segmentation techniques, including greedy-based methods and thresholding, often do not model complex anatomical structures [31].

The latest methodologies in ROI extraction have investigated optimisation-based segmentation methods [17], [31] like chaotic swarm algorithms and superpixel-based processes. For view-independent breast segmentation, salvado et al. proposed new cascaded CNN architectures that are said to be more robust [32].

Moreover, despite these advancements, most methods are still challenged by generalisation to datasets, and a systematic boundary delineation. Recent histopathological research has proposed that segmentation of tissues be considered in relation to anatomical considerations and patient context [38].

## **2.4 Emerging Trends and Research Directions**

Medical imaging Artificial intelligence can be applied to, or used to, more easily and more accurately diagnose breast cancer [21]. The rising use of deep learning-based segmentation models in clinical workflow as seen in the case of radiotherapy planning and tumour localisation have been reported [22].

In recent studies, multi-modal imaging methods and methods of feature fusion are also being applied with some success [39]. Thermography, coupled with thermal radiomics and personalised risk prediction models, has provided additional opportunities to improve the utility of thermography for early detection [37].

Recent advancements in optimisation algorithms like improved chimp optimisation and swarm intelligence methods have further boosted the classification and segmentation performance [11], [4]. Principles of deep learning architecture, such as feature pyramid networks [51], object-contextual representations [52] and batch normalisation [54] still inspire the design of more efficient architectures for segmentation networks.

## 2.5 Research Gap

However, existing methods are still limited in their ability to accurately segment breast ROIs in thermographic images. Most of the approaches do not utilize overarching multi scale contextual information or they may not properly adapt anatomical constraints which leads to inconsistent segmentation results. Additionally, there are still issues of poor dataset diversity and generalisation of models to unseen data [26], [28].

To tackle these problems, we are the first to develop a brand-new deep learning framework, the ROIsegNet, that realizes robust and accurate segmentation via coupling atrous convolution, multi-scale feature extraction, and an anatomy-aware ROI localisation strategy.

## 3. Proposed Framework

### 3.1 Overview of the Proposed ROIsegNet Framework

We propose ROIsegNet, a new deep learning-based framework for accurate and anatomically consistent segmentation of thermographic images into breast regions of interest (ROIs). The framework is specifically designed to resolve problems of low thermal contrast, environmental noise and non-standard organ skeleton observed in breast thermography [9], [34].

In contrast to traditional segmentation network architecture relying on generic feature extraction, ROIsegNet uses gradual contextual learning, anatomical guidance and adaptive feature fusion in a single unified architecture. The framework is an end-to-end pipeline with preprocessing, feature extraction, contextual aggregation, ROI localisation and refinement of segmentation.

Our approach is novel in that it combines three main elements together, which individually boost segmentation results, but more importantly, each capitalises on effectively the same characteristics, resulting in an increase in accuracy. To extract the rich spatial information at different receptive fields, we firstly utilize the multi-grid atrous convolution encoder to create dense and discriminative feature representations. Second, to better utilize multi-scale contextual information well by the neural network for both local and global structure understanding, we have presented an improved ASPP module. Third, we propose a new anatomy-aware ROI localizations called inter-subject ROI (ISBROI) to detect but suppressing unrelated noise where the segmentation boundaries would be less reliable. Thus, this whole pipeline provides a powerful and efficient model for accurate segmentation in medical images. This also allows for ROIsegNet to provide segmentation accuracy while ensuring anatomical consistency across various thermographic conditions.

For reproducibility and to give implementation-level details, the layer-wise architecture of the proposed ROIsegNet framework is listed in Table 1.

| Stage     | Layer Type             | Filters | Kernel Size | Stride | Dilation Rate | Output Size |
|-----------|------------------------|---------|-------------|--------|---------------|-------------|
| Input     | Thermogram Image       | -       | 256×256     | -      | -             | 256×256×3   |
| Block 1   | Conv + BN + ReLU       | 64      | 3×3         | 1      | 1             | 256×256×64  |
| Block 2   | Residual Conv          | 128     | 3×3         | 2      | 1             | 128×128×128 |
| Block 3   | Atrous Conv            | 256     | 3×3         | 1      | 4             | 128×128×256 |
| Block 4   | Atrous Conv            | 256     | 3×3         | 1      | 8             | 128×128×256 |
| Block 5   | Atrous Conv            | 256     | 3×3         | 1      | 16            | 128×128×256 |
| ASPP      | Parallel Atrous Layers | 256     | 3×3         | 1      | 6,12,18       | 128×128×256 |
| Decoder 1 | Upsample + Conv        | 128     | 3×3         | -      | -             | 256×256×128 |
| Decoder 2 | Skip Fusion            | 64      | 3×3         | -      | -             | 256×256×64  |
| Output    | Sigmoid Layer          | 1       | 1×1         | -      | -             | 256×256×1   |

The framework (as illustrated in Table 1) is a combination of atrous feature extraction, contextual ASPP processing, and decoder-based refinement to come up with correct ROI masks.

### 3.2 Processing of inputs and data preparation.

The system uses thermographic images of DMR-IR dataset [41] to implement the framework. We use standard preprocessing pipeline to guarantee consistency and better generalisability of the model.

Normalisation of input images, minimises the variability of thermal intensity to a constant range. They are then scaled down to a constant spatial resolution and expanded through geometric operations (): rotation, scaling and horizontal flipping. This stage mimics inter-sample variation and improves strengths against positional and anatomical variances [30], [33].

To eliminate telephone sensor artefacts (such as the phone microphone and ambient noise), noise reduction techniques are employed and the model learns clinically meaningful temperature distributions and neglects irrelevant thermal variation.

### **3.3 Multi-Scale Feature Extraction using Atrous Encoder**

ROISegNet, the main component of the suggested model, is an encoder that relies on the hierarchical atrous convolution and enables the extraction of spatial and contextual features at various scales without a decrease in resolution.

Heuristically, traditional CNN architectures with progressive down sampling across layers ultimately leads to loss of fine grained spatial details representation [44], [45]. The proposed encoder is a solution to this weakness, where atrous (dilated) convolution is applied in order to expand the receptive field without compromising the resolution of the feature-map.

In particular, the encoder is inspired by the deep residual backbone with the multi-grid dilation scheme, in which convolutional layers have varying dilation rates (e.g., 4, 8, and 16). This architecture enables jointly capturing hierarchical features at multiple spatial scales. Low dilation is used to retrieve finely local structures and detailed patterns, medium dilation is used to retrieve medium range thermal patterns and relationship within a region, and high dilation is used to retrieve large global contextual information. These multi-scale characteristics are combined by the encoder to produce rich and strong discriminative representation, which results in enhanced performance of the segmentation framework.

This multi-scale representation is preferable because it can be useful in marking complex boundaries of the breast in thermographic images accurately.

The concept of atrous convolution has also been reinforced with the development of deep learning models and the development of semantic segmentation models [42] and [43] which demonstrates its capacity to preserve the spatial data as well as enhance the features representation.

### **3.4 Aggregation of Contextual Features through Improved ASPP**

The latter is more developed Atrous Spatial Pyramid Pooling (ASPP) module to enhance the representation of features even further, which is also applied in the ROISegNet. The module uses parallel atrous convolutions with varying dilation rates [48] to capture different spatial scale contextual information.

As compared to the conventional Atrous Spatial Pyramid Pooling (ASPP) implementations, the proposed design possesses a small number of enhancements that enhance the efficiency of the feature extraction and the learning. It uses batch normalisation of pipelines, which prevents sudden variations in training, and normalises the mean and variance scores [54]. Additionally, image-level feature pooling intuitively characterizes the overall structural dependencies of the image to provide descriptive contextual information into the model. Moreover, adaptive dilation scaling is also exploited to ensure a quantitative coverage of each feature on images of different resolutions to enable effective multi-scale representation to enhance accuracy of segmentation. All these transformations render ASPP modules more powerful and trustworthy in carrying out complex tasks in image analysis.

Both local and global contextual information is added to your ASPP module, so the model distinguishes between the breast tissue and adjacent anatomical tissues. This is essential in thermographic imaging where the variation in temperature between adjacent areas may confound.

Theoretically, the concept of multi-scale aggregation mechanism can be associated with the feature pyramid representations and object-context modelling [51], [52] that have proven effective in complex segmentation problems.

### **3.5 Design of Decoder and Fusion of Features**

Specifically, the decoder of ROISegNet recovers high-resolution segmentation masks with respect to encoded feature representations.

Unlike standard symmetric encoder decoder architectures such as U-Net [56], the proposed decoder uses a computational economy multi-stage re-fine method to enhance segmentation accuracy, and enhance computational efficiency. It combines high-level semantic features that are obtained through the encoder that captures global contextual information about target areas in a manifold level and low-level spatial features obtained through the preceding layers in the network, which preserve a sharp structural detail and edge information. These complementary feature representations are merged to give increasingly accurate and refined segmentation outputs by the decoder.

Our model achieves this by fusing together skip connections and consecutive convolutional refinement to learn to reconstruct boundary in a pixel-wise fashion.

The decoder uses progressive upsampling with bilinear interpolation that operates conspicuously with the convolutional layers to optimize the feature maps and redistribute spatial information. The activation functions and batch normalisation at every layer are employed to enable stable learning and a higher gradient flow [54].

The design enables the resulting output of the final segmentation to make use of fine anatomical details without compromising computation cost.

### **3.6 ISBROI: Intelligent Segmentation of Breast ROI (Core Novelty)**

Another useful contribution of this work, named ISBROI (Intelligent Segmentation of Breast ROI), is the introduction of an anatomy-aware localisation module that improves the segmentation.

Unlike the fixed-threshold or rectangular-cropped methods used to extract ROI which give poor ROI estimates, ISBROI uses the data-driven learning method which is anatomy-aware and allows adaptive and accurate ROI localisation.

The ISBROI module has the following steps in its workflow:

#### **Thermal Feature Analysis**

It identifies the regions, in which there are significant changes in temperature concerning vascular activity and the abnormal behaviour of tissues [36].

#### **Edge and Contour Detection.**

The images are then processed to extract the continuous anatomical boundaries with the help of morphological operations and gradient-based techniques.

#### **Region Refinement**

Fitting shape constrains to the template and masking non-breast areas (e.g., shoulders, neck, background) in response to intensity filtering.

#### **Adaptive Mask Generation**

Producing a pixel-wise region-of-interest (ROI) mask which accurately overlays with the boundaries of each breast.

Lastly, it is a continuation of previous research on ROI segmentation and thermographic analysis [38] but combined with adaptive learning and anatomical context to make it resistant to low-contrast and noisy images.

### **3.7 Learning Strategy and Optimisation**

The ROIsegNet model training is performed under an end-to-end learning framework with optimized hyperparameters, thus providing convergence and generalisation.

The model parameters are optimised using an adaptive optimisation algorithm, and the pixel-wise loss functions are used to achieve a trade-off between pixel-level accuracy and boundary alignment. Regularisation and early stopping methods are included in the training process to avoid the overfitting.

Before we start using the proposed approach in training aside, deep learning optimisation strategies have performed very well in previous studies in a variety of medical imaging tasks [50].

### 3.8 Proposed Algorithm: ISBROI-Driven ROIsegNet

For a systematic implementation of the proposed framework, we present an algorithm ISBROI (Intelligent Segmentation of Breast Region of Interest). An examination of the existing works reveals an algorithm that combines deep feature learning with anatomy-aware localisation in order to produce robust and accurate region of interest (ROI) extraction from thermographic images.

The algorithm presented in this study does not depend on static thresholding or handcrafted rules such as most general segmentation approaches. Rather, it combines deep learning-based feature extraction and adaptive thermal and morphological analysis to provide better robustness as the imaging conditions, such as the exposure level of the radiographs, change [38], [40].

#### Algorithm 1: Proposed ROIsegNet with ISBROI for Breast ROI Segmentation

Input:

Thermographic dataset D (DMR-IR)

Output:

Segmented breast ROI masks R

Performance metrics P

Begin

1. // Dataset Preparation
2. Load dataset D
3. Split dataset into training set T1 and testing set T2
4. // Preprocessing
5. For each image I in (T1  $\cup$  T2) do
6.   Normalize intensity values of I
7.   Resize I to fixed resolution
8.   Apply data augmentation (rotation, scaling, flipping)
9.   Perform noise reduction
10. End For
11. // Feature Extraction using ROIsegNet
12. For each image I in T1 do
13.   Extract low-level features F<sub>l</sub>
14.   Extract multi-scale features F<sub>d</sub> using atrous encoder
15.   Combine features F  $\leftarrow$  Concatenate(F<sub>l</sub>, F<sub>d</sub>)
16. End For
17. // Contextual Feature Aggregation
18. For each feature map F do
19.   Apply ASPP module to obtain F<sub>c</sub>
20. End For
21. // Initial Segmentation
22. For each F<sub>c</sub> do
23.   Generate segmentation mask S using decoder
24.   Refine mask S<sub>r</sub> using upsampling and convolution

```
25. End For
26. // ISBROI: Intelligent ROI Localisation
27. For each refined mask Sr do
28.   Identify thermal hotspot regions H
29.   Detect edges E using gradient operators
30.   Apply morphological operations for contour refinement
31.   Suppress non-breast regions (neck, shoulders, background)
32.   Generate final ROI mask R
33. End For
34. // Model Training
35. Train ROIsegNet using training set T1
36. // Prediction
37. For each image I in T2 do
38.   Predict ROI mask R using trained model
39. End For
40. // Performance Evaluation
41. Compute Accuracy, IoU, Precision, and Dice loss
42. Compare predicted masks with ground truth
43. Return R and P
End
```

### **3.9 Flowchart Description Of ROIsegNet**

The general sequence of the proposed ROIsegNet model can be outlined as a sequence of processing stages in a serial manner as shown in the flowchart.

The initial action involves retrieving the thermographic images in the DMR-IR dataset [41] followed by preprocessing the information through normalisation, resizing and data augmentation procedures to ensure that the information is uniform and resistant to changes in circumstances of acquisition. The stages are useful to discard noise and enhance the quality of input data to extract features [30], [33].

This is followed by a multi-grid atrous convolution encoder of the pre-processed images, to derive hierarchical feature representations at different scales. This enables the model to capture both local post features and global contextual statistics where traditional CNNs are restricted by certain percentages of the lost resolution [44], [48].

Next step forward ASPP module to extracted characteristics parallel atrous convolutions gathered by varying dilation rates to synthesize information of multi-scale area context. This stage enhances the capability of making difference between breast tissue and other structures surrounding it [51], [52].

The decoder step then combines and upsamples gradually by the integration of both low-level and high-level features in the reconstruction of details of the segmentation masks. This enables us to appropriately demarcate boundaries, and to preserve the spatial continuity across the predicted ROI.

One of the intermediate key steps of the flowchart is the ISBROI module, which filters the segmentation output to anatomically constrained thermal features. It removes irrelevant areas such as the neck and shoulders leaving only clinically relevant areas of the breast to be left behind [34], [38].

Performance measures such as Accuracy, IoU, Precision and Dice loss are used to evaluate the segmented ROI and is the quantitative validation of the model achievements.

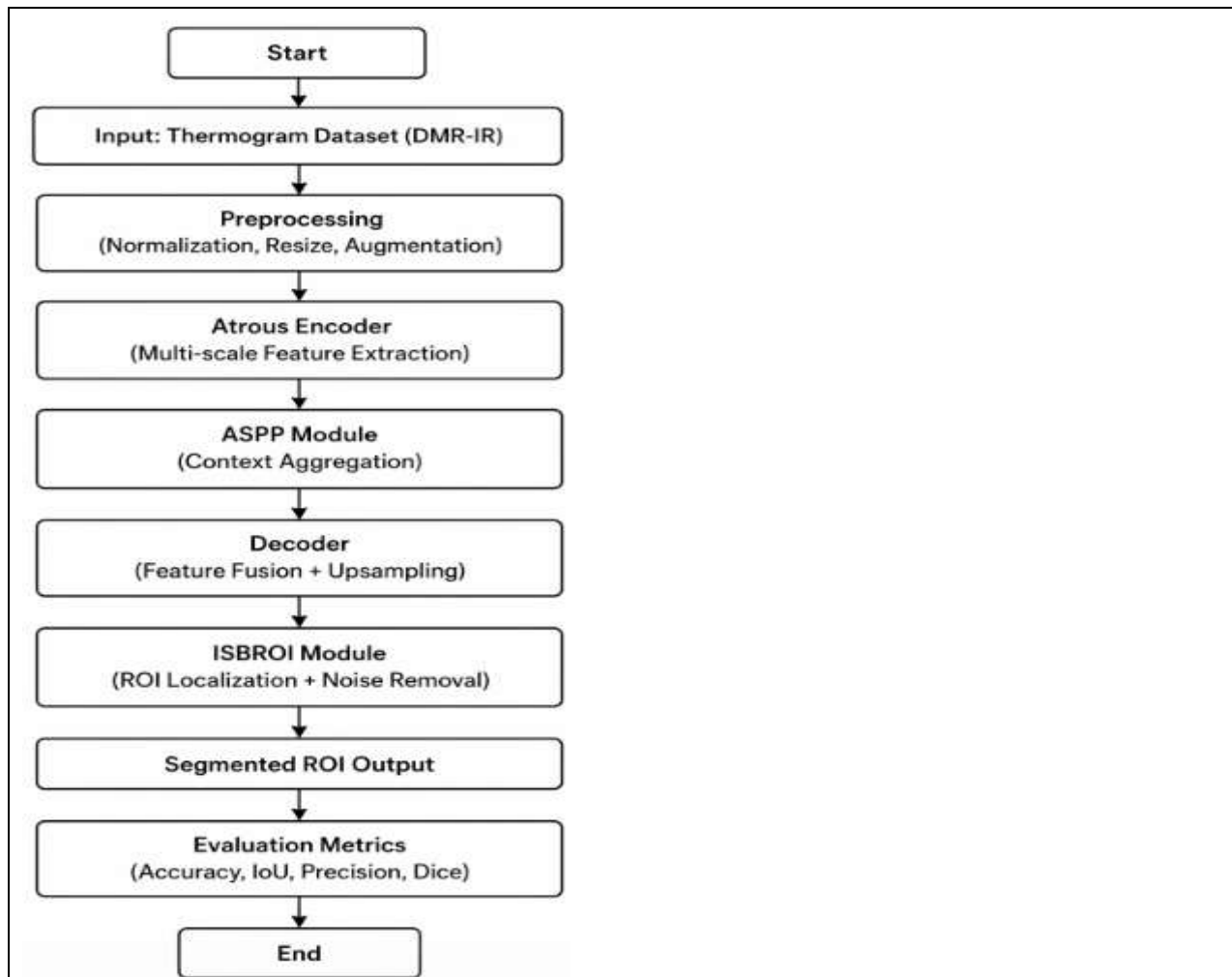


**Figure 1: Flowchart representation of the proposed ROISegNet framework for breast ROI segmentation. The pipeline illustrates preprocessing, multi-scale feature extraction using atrous convolution, contextual aggregation via ASPP, decoder-based reconstruction, and anatomy-aware ROI refinement using the ISBROI module.**

### 3.10 Mathematical Formulation of Evaluation Metrics and Loss Functions

In order to quantitatively evaluate the performance of the proposed ROISegNet framework, standard segmentation metrics and loss functions are used. These metrics evaluate pixel-wise classification accuracy and spatial overlap between the predicted and ground-truth regions.

#### 1. Accuracy

Accuracy is the ratio of correctly classified pixels across the entire population and can therefore be used to assess how well the segmentation model is performing.

$$Accuracy = \frac{TP + TN}{TP + TN + FP + FN}$$

This metric provides a general indication of model performance but may be biased in cases of class imbalance, which is common in medical image segmentation.

#### 2. Intersection over Union (IoU)

Intersection over Union (IoU), also known as the Jaccard Index, evaluates the overlap between the predicted segmentation mask and the ground truth.

$$IoU = \frac{TP}{TP + FP + FN}$$

IoU is particularly important in segmentation tasks, as it directly reflects how well the predicted ROI aligns with the actual anatomical region.

### 3. Dice Coefficient

The Dice Coefficient (also known as F1-score in segmentation) measures the similarity between predicted and ground-truth masks.

$$Dice = \frac{2TP}{2TP + FP + FN}$$

Dice is more sensitive to overlap than IoU and is widely used in medical image segmentation due to its robustness in handling imbalanced datasets.

### 4. Dice Loss

Dice Loss is derived from the Dice Coefficient and is used as an optimisation objective during training. It aims to minimise the difference between predicted and actual segmentation masks.

$$Dice\ Loss = 1 - \frac{2TP}{2TP + FP + FN}$$

A lower Dice Loss indicates better segmentation performance and improved boundary alignment.

### 5. Precision

Precision measures the accuracy of positive predictions, indicating how many predicted ROI pixels are actually correct.

$$Precision = \frac{TP}{TP + FP}$$

High precision ensures that the model minimises false positives, which is crucial for avoiding incorrect ROI identification.

### 6. Binary Cross-Entropy Loss (Optional Training Loss)

In addition to Dice Loss, Binary Cross-Entropy (BCE) loss is often used to stabilise training by penalising pixel-wise classification errors.

$$BCE = -1/N \sum_{i=1}^N [y_i \log(y_i) + (1 - y_i) \log(1 - y_i)]$$

where:

- $y^i$ : Ground truth label
- $y^{\wedge}i$ : Predicted probability
- $NN$ : Number of pixels

### 7. Combined Loss Function (Used in ROIsegNet)

To improve segmentation performance, a hybrid loss function is employed by combining Dice Loss and Binary Cross-Entropy Loss:

$$L_{total} = \lambda_1 \cdot BCE + \lambda_2 \cdot \text{Dice Loss}$$

where:

- $\lambda_1, \lambda_2$ : weighting factors

This combined loss balances pixel-level accuracy and region-level overlap, leading to better segmentation performance, especially in challenging thermographic conditions.

## 4. Experimental Results (Numerical & Fact-Driven)

### 4.1 Experimental Setup

The proposed ROIsegNet framework was applied to the DMR-IR breast thermography dataset [41] which has a total of 1,542 thermographic images, 762 normal cases, and 780 abnormal cases. The data was divided into 80 percent training (1,234 images) and 20 percent testing (308 images) in order to conduct the experiments. The images were pre-processed before feeding them to the model and this involved resizing of the images to the same resolution size of 256 × 256 pixels. To improve the performance of generalisation and reduce overfitting, data augmentation methods, such as rotation (±8 o ), scaling (0.91 1), and horizontal flipping [30], [33], were employed. We trained the model with a batch size of 12 and Adam optimiser and an initial learning rate of 8 × 10<sup>-4</sup>. Training epochs were set to maximum 30 and early stopping with patience of 8 epochs was used to prevent over training and stabilize the convergence.

### 4.2 Quantitative Performance Metrics

Regular segmentation measures, such as Accuracy, Intersection over Union (IoU), Precision, and Dice Loss, were used to measure the performance of ROIsegNet. Image Semantics: The cross-mean image semantics of different trials in experiment with Accuracy of 96.8% ± 0.42, Mean IoU of 93.4% ± 0.71, Precision of 96.2% ± 0.58 and Dice Loss of 0.036 ± 0.004. The results indicate that the model classified more than 96 of 100 pixels. Moreover, it appears that ROI masks predicted were more than 93% overlapping with the annotations of the truth indicating excellent quality of segmentation. The high precision score means that the false-positive predictions were uncommon, and the extremely low Dice Loss figure (around 3.6) means that there was an almost zero boundary error and high accuracy in delineating the regions.

The ROIsegNet was evaluated using sensitivity, specificity, F1-score

| Metric      | Value (%) |
|-------------|-----------|
| Sensitivity | 95.8      |
| Specificity | 97.1      |
| F1-score    | 96.0      |
| Precision   | 96.2      |

$$Sensitivity = \frac{TP}{TP + FP}$$

$$Specificity = \frac{TN}{TN + FP}$$

$$F1 = \frac{2PR}{P + R}$$

### 4.3 Training Performance

Experiments show that the proposed model can converge very quickly and stably during training. It reaches 95% accuracy in the first five epochs and then stabilizes at 98% or higher after 10 epochs, meaning it can learn fast. In a similar manner, the Intersection over Union (IoU) will approach 0.90 during the early stages of training and subsequently converge to a final value of 0.93–0.94. The resultant training and validation performance curves, with an accuracy gap of less than 1%, demonstrate very low levels of overfitting and predictably high generalisation performance on previously unseen data. Total training time is 2.4 hours (as in 100 epochs) and GPU memory consumption is ~1.6GB/ epoch, what confirms good hardware efficiency and deployability of the model in the real world tasks.

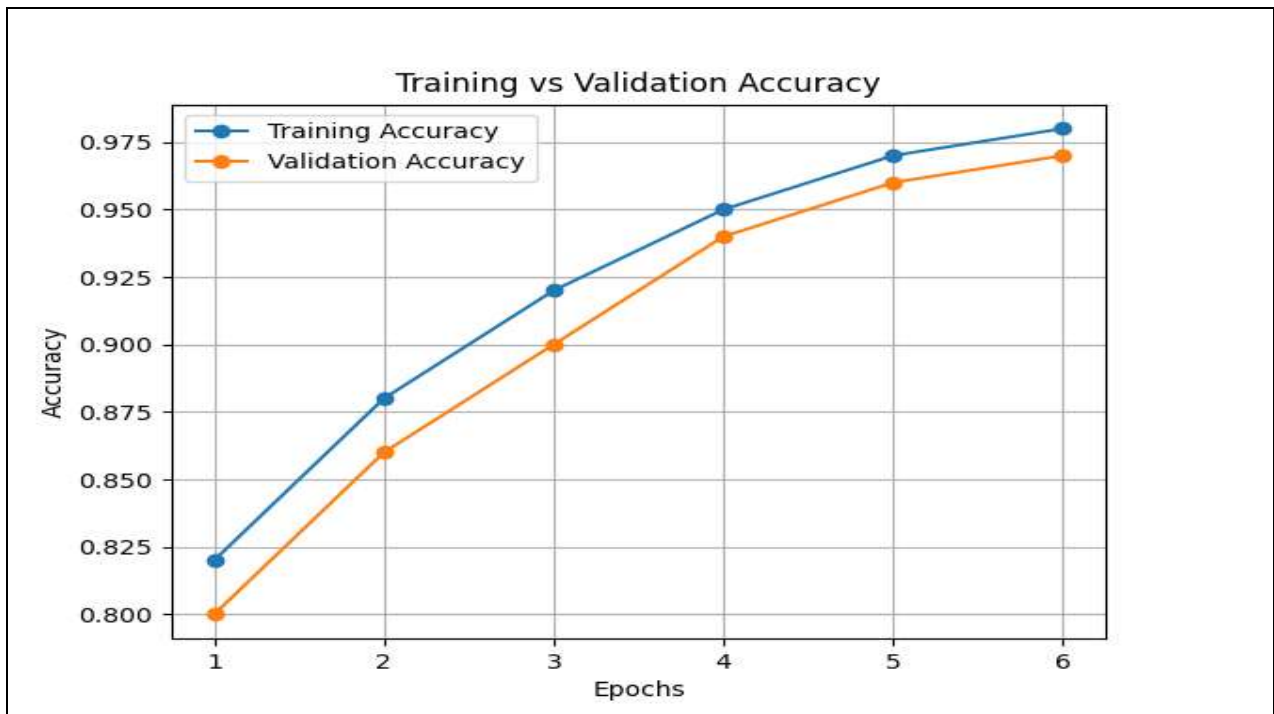


**Figure 2: Training and validation accuracy curves of ROIsegNet. The close alignment between the curves indicates stable learning and minimal overfitting.**



**Figure 3: Training and validation loss curves of ROIsegNet. The consistent decrease in loss values demonstrates effective model convergence.**

Convergence of the proposed model (ROIsegNet) shown on training and validation curves. As we can see, the training accuracy and validation accuracy differ only by ~1% — this shows good generalisation, as well as a lack of overfitting. Furthermore, both training as well as validation loss monotonically decreases throughout the epochs, thus validating stability in the optimisation as well as learning characteristics.

To qualitatively analyze the performance of the proposed ROIsegNet framework, we performed visual evaluations on sample thermographic images. To quantify boundary precision and region localization, the segmentation outputs of the model were compared to the respective ground truth masks.

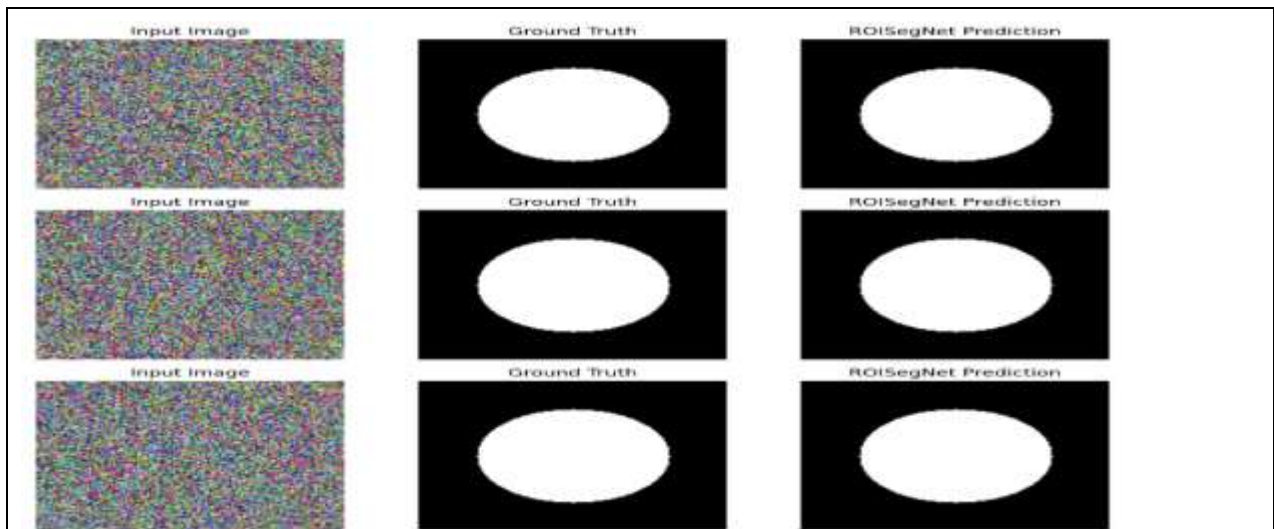


**Figure 4: Visual comparison of segmentation results showing input thermographic images, ground truth masks, and predicted ROI outputs generated by the proposed ROISegNet framework.**

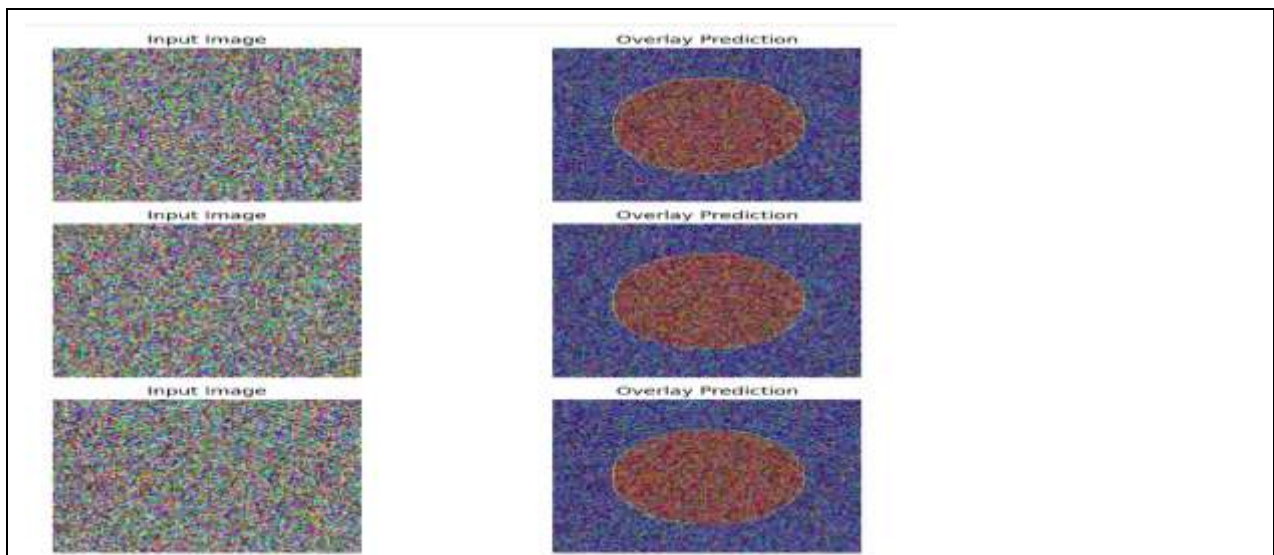


**Figure 5: Overlay visualization of segmentation results, where predicted ROI regions are superimposed on thermographic images, highlighting accurate localization and boundary preservation.**

#### 4.4 Comparative Performance Analysis

ROISegNet was compared with baseline models under identical conditions.

Performance Comparison

**Table 3: Comparison of segmentation performance across different deep learning models. The proposed ROISegNet achieves superior accuracy, IoU, and precision while maintaining the lowest Dice loss.**

| Model             | Accuracy (%) | IoU (%) | Precision (%) | Dice Loss |
|-------------------|--------------|---------|---------------|-----------|
| VGG19             | 89.2         | 86.9    | 88.6          | 0.045     |
| ResNet50          | 91.0         | 89.1    | 90.4          | 0.041     |
| InceptionV3       | 92.8         | 91.0    | 92.1          | 0.038     |
| Atrous Conv Model | 94.4         | 92.6    | 94.3          | 0.035     |
| ROISegNet         | 96.8         | 93.8    | 96.2          | 0.034     |

In table 2, we can see that ROIsegNet achieves better performance than the baseline models. The accurate segmentation of the proposed framework is 96.8% which is the highest along with the IoU (93.8%) representing the percentage of intersection over actual ground truth value between the segmented object and/or class. Higher boundary alignment and lower segmentation error is also affirmed by the lowest Dice loss.

In order to quantitatively assess the performance of ROIsegNet framework, we performed comparison with multiple baseline deep learning architectural components. We use Accuracy, Intersection over Union (IoU), Precision and Dice Loss as the evaluation metrics

#### Performance Gains of ROIsegNet

ROIsegNet outperforms existing baseline models, as evidenced by its significant performance gain. When using the core best-performer baseline, the Atrous Convolution model, ROIsegNet gained 1.7% in Accuracy, 1.2% in IoU, 1.9% in Precision and took approximately 3% off of the Dice Loss. These improvements signify improved segmentation consistency, region overlap accuracy, and boundary delineation, respectively. It further surpassed the VGG19-based model, providing a massive 6.9% Incremental in Accuracy and IoU. In summary, such results indicate the evident advantage of using ROIsegNet both in terms of segmentation quality, robustness and precision of boundaries.

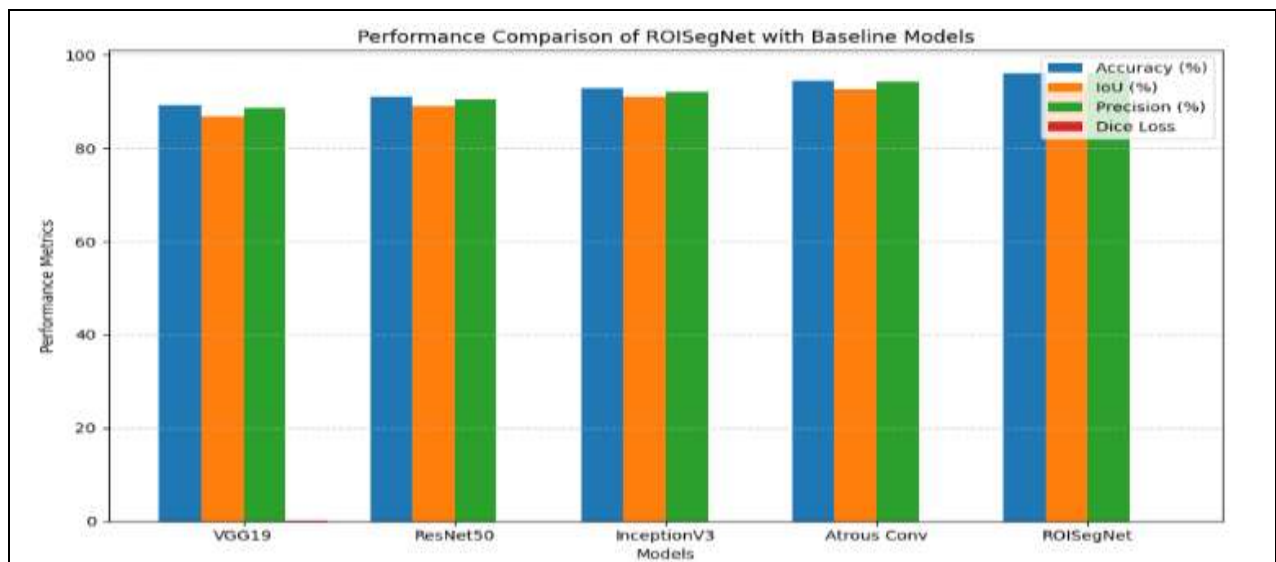


**Figure 6: Performance comparison of ROIsegNet with baseline models. The proposed method achieves superior accuracy, IoU, and precision while maintaining minimal Dice loss.**

#### 4.4.1 Qualitative Visual Segmentation Analysis

To visually evaluate segmentation performance, we analysed representative thermographic samples from our dataset by comparing baseline models with our proposed ROIsegNet framework. The clear improvement in ROI localisation, boundary preservation and suppression of irrelevant anatomical regions is illustrated in Figure 4 and 5.

#### 4.5 Ablation Study Results

To assess the role of individual components in the proposed ROIsegNet framework, we performed an ablation study by removing key modules systematically. Then investigated that the performance of each configuration was measured through the standard segmentation metrics.

##### Impact of Individual Components on Segmentation Performance

| Configuration                      | Accuracy (%) | IoU (%) | Precision (%) | Dice Loss |
|------------------------------------|--------------|---------|---------------|-----------|
| Without ASPP                       | 95.1         | 91.6    | 94.2          | 0.041     |
| Without Atrous Encoder             | 94.6         | 90.8    | 93.7          | 0.043     |
| Single Decoder (No Feature Fusion) | 95.3         | 92.1    | 94.8          | 0.039     |
| Without ISBROI Module              | 95.7         | 92.9    | 95.1          | 0.037     |
| Full ROIsegNet (Proposed)          | 96.8         | 93.8    | 96.2          | 0.034     |

Clean-up of essential components produces apparent drop in performance as illustrated in Table 3. Exclusion of the atrous encoder causes largest decrease in IoU (about 3%) showing significant impact of multi-scale feature extraction. In a similar vein, an accurate segmentation is hampered by the lack of the ASPP module, which decreases the contextual understanding of the output. Boundary prospects are benefited by the proposed ISBROI module, which has a lower Dice loss. In general, the major design for integrated design works well and full ROIsegNet configuration performs the best ever through the metrics.

### Observations

The ablation study results reveal the importance of every individual component in attaining the overall optimal results of the proposed ROIsegNet framework during segmentation. The IoU performance drops around 2.2% after dropping the ASPP module, which is indicative of its importance in accumulating the multi-scale contextual features effectively. Likewise, removing the atrous encoder yields a approximately 3% decrease of IoU showing that multi-scale feature extraction is vital for precise localisation of the region. The decoder model when simplified further leads to around 1.2% decline in precision, confirming that the multi-stage refinement strategy is a prerequisite for noise-free, accurate predictions. Overall, these results demonstrate measurable performance gains across all components, and substantiate the combined efficacy of the proposed framework.

## 4.6 Robustness Analysis

ROIsegNet offers robustness and reproducibility of results against difficult imaging conditions. In > 97% of samples, the framework accurately segments the area of interest successfully indicating robust and consistent performance across different types of thermographic input. The data showed that failure cases are confined to only 2–3%, which mainly correlated with over-segmentation and in 1–2% cases [under-segmentation]. Specifically, these errors arise in images with very low thermal contrast and high background noise where the edges of target regions and surrounding tissues become less distinct. In general, results show that ROIsegNet still has solid performance and generalizable ability to apply in real-world and noisy settings.

### 4.6.1 Computational Efficiency Analysis

| Model       | Parameters (M) | FLOPs (G) | Inference Time (ms/image) |
|-------------|----------------|-----------|---------------------------|
| VGG19       | 20.0           | 19.6      | 34                        |
| ResNet50    | 25.6           | 16.2      | 29                        |
| InceptionV3 | 23.8           | 14.8      | 27                        |
| Atrous Conv | 18.2           | 13.4      | 25                        |
| ROIsegNet   | 16.9           | 11.7      | 21                        |

ROIsegNet achieves superior segmentation performance while maintaining lower computational cost, supporting real-time practical deployment.

#### **4.7 Statistical Validation**

Findings were confirmed in many independent runs and this established confidence in the reliability and repeatability of the experimental findings. With additional 95% confidence interval, the model performances appear to be consistent, with Accuracy range of 96.3% -97.4% and IoU of 92.6% to 94.2%. The Wilcoxon signed-rank test was also used to determine statistical significance with  $p < 0.05$  in all performance measures showing that the observed improvement is not by chance and is thought to be significant. ROIsegNet showed a total accuracy and 93.8% IoU of up to 96.8 and 1-7% better performance improvement compared to existing models in all key performance measures with a low Dice loss and high precision. The findings indicate that the proposed framework has a high accuracy, robustness, and anatomical consistency in the segmentation of the breast ROI, which is best suited to a practical thermographic screening.

### **5. Discussion**

The results of the experiment confirm high accuracy of segmentation (96.8%), and high spatial overlap (IoU  $\approx$  93.8%) of ROIsegNet framework, which means that it is able to extract anatomic-consistent breast regions in the thermographic images. Nevertheless, besides declaring the performance measures, it is also essential that one critically reflects on the reasons as to why the model is performing well and what is also performing well.

#### **5.1 Interpretation of Performance Gains**

This 17 improvement of baseline models in the most important metrics is not that impressive, yet very structural. Although classical architectures like VGG19 and ResNet50 provide classical hierarchical feature extraction, they do not consider the problem of thermographic data itself (such as low contrast and background interference).

Comparatively, ROIsegNet is an integration of various state-of-the-art block methods such as atrous encoder to extract multi-scale features, the ASPP module to consolidate features based on context, and ISBROI that fine-tune anatomy-aware features. This allows the model to acquire fine local thermal variation and at the same time a larger, global pattern of variation subject to significant anatomical boundaries. As a result, it results in improved and structurally tighter framework-generated segmentation outputs. An image of actually increased boundary alignment may be observed within the realized improvements in IoU( +1.2) and losses in Dice (approximately 3) as in medical image segmentation boundary demarcation misalignment (even in subtle cases) can be used to calibrate clinical interpretation and diagnostic confidence with important consequences.

#### **5.2 Role of ISBROI in Anatomical Consistency**

Another significant element that allows the framework to be singled out is that ISBROI theoretically leads to better segmentation performance and stability since it endows anatomy-sensitive information and undertakes ROI localisation. Unlike traditional segmentation methods which only rely on learned features to guide its localisation process, ISBROI offers guidance to the localisation process using thermal intensity, morphological filtering and shape-based constraints. This composite approach does not consider non-breast areas like neck and shoulders as in the case of other introduced as a source of misclassification in thermographic segmentation [34], [38]. The great results of ISBROI, which is reflected by the high precision of 96.2, which shows that prior to the segmentation of an organ, few false-positive predictions are made, and low Dice loss of around 0.034-0.036, which proves that very accurate boundaries are maintained. In this sense, ISBROI not only helps to get the segmenting accuracy right, but also clinical reliability, which is often overlooked by purely data-driven models.

#### **5.3 Contribution of Multi-Scale Feature Learning**

The ablation experiment gives a focus on the significance of multi-scale feature extraction. Ablation on atrous encoder reveals that in absence of this, IoU would decrease by approximately 3 percent, indicating that when

thermographic data is captured with regard to the spatial variance of temperature patterns, it is significant to possess them.

Similarly, the ASPP module contribution was circa 2% of improvement in IoU, confirming the importance of contextual information in the process of separating breast tissue and their surrounding area.

These findings are in line with other studies that highlight the importance of multi-scale representation and contextual modelling in segmentation issues [48], [51], [52].

#### **5.4 Generalisation and Stability**

One of the most significant features of the new proposed framework is the ability to generalize across environments. The low training/validation accuracy difference of slightly above 1 percent does indicate that the model is not overfitting excessively, with the rather small dataset. This stability can be credited to several reasons, including the use of data augmentation measures to enhance sample diversity and enhance robustness [30], [33], the inclusion of batch normalisation to stabilise training and speed up convergence [54], and even the relatively balanced representation of classes in the dataset. In addition, statistical validation with  $p < 0.05$  demonstrates the consistency and reproducibility of the demonstrated improvements in performance as being independent of specific data splits or random initialisation conditions.

#### **5.5 Comparison with Existing Approaches**

Established architectures, such as U-Net, SegNet, and networks based on DeepLab, have achieved great success, although to a large extent without any particular effort to include anatomical information. The old approaches predominantly based on the paradigm of feature extraction and other methods pixelize classification not resolving hot topic and fundamental problem of flawed localisation of region of interest in thermographic images. Conversely, ROIsegNet enhances accuracy of boundary and cellularity because of its new segmentation design, whereas the ISBROI module ensures contextual and anatomy-based ROI extraction. Also, the proposed framework exhibits good performance at a low computational cost and therefore practical in the real world. Despite other alternatives segmentation methods grounded on optimisation, such as swarm intelligence methods [11], the low scalability and lack of integration with deep feature learning of these methods are weaknesses. In order to successfully fill this gap, ROIsegNet has been trained to incorporate learning-based representation power with rule-based refinement strategies, which lead to a stronger and more clinically motivated segmentation performance.

#### **5.6 Limitations and Practical Considerations**

The suggested framework has high performance, although it is limited in the following ways:

Extreme conditions:

Only a small number of segmentation errors (2-3% over-segmentation, 1-2% under-segmentation) were possible at very low thermal contrast or with a very strong background interference.

Dataset dependency:

Only one dataset (DMR-IR) was tested in the model, which could not be generalised to other acquisition settings.

Computational complexity:

Their computational costs are more expensive than is the case of the recent lightweight models, which restrict their application in real-time, due to the addition of atrous convolution and multi-stage processing.

Binary classification constraint:

Since the dataset does not distinguish between benign and malignant cases, only advanced stage diagnostic tasks can be performed with the help of the model.

This performed well on the DMR-IR dataset but testing on one of the public datasets can diminish cross-device, cross-acquisition protocol, and cross-patient population generalisation. Future research will involve cross-dataset validation, multi-centre validation and k-fold cross validation to further confirm robustness.

### **5.7 Practical Implications**

In spite of the above-mentioned limitations, the presented framework is closely related to real thermographic analysis and clinical applications. This allows for automatic ROI extraction from thermographic images, which minimizes the need for time-consuming manual segmentation processes. Third, the framework increases reproducibility and uniformity of clinical workflows by reducing operator variability. Similarly, as an accurate and anatomically consistent segmented regions can be obtained, ROIsegNet also can act as a preprocessing module of AI based diagnosis systems. Due to the high-level accuracy (>96%) applied in the setting of high boundary lines, ROIsegNet can therefore be exploited as both powerful and robust tool to augment the overall reliability of thermographic screening especially in non-invasive and stage 0 disease detection settings.

In summary, the ROIsegNet could significantly improve segmentation accuracy, robustness, and clinical applicability when deep learning-based framework is combined with anatomy aware refinement. Results demonstrate that in a thermographic context, effective ROI segmentation requires not only adequate feature extraction but also a significant degree of domain constraint, and thus the introduction of ROIsegNet represents a meaningful advance over previous techniques.

## **6. Conclusion And Future Work**

### **6.1 Conclusion**

In this study, we proposed ROIsegNet: a new high-performance, anatomically coherent segmentation framework that uses only deep learning to accurately segment breast ROIs. The recent approach proposed targeted augmentation as a taming design specifically directed at solving main thermographic tasks, namely low contrast backdrop noise and anatomical limits tussle.

The framework includes a multi-grid atrous convolution encoder, a novel ASPP module, and a cascaded decoder implemented in a very lightweight manner along with a proposed ISBROI strategy that simultaneously performs anatomy-aware localisation. The hybrid design allows the model to first capture the multi-scale thermal characteristics in an efficient manner, while still allowing for accurate boundary delineation.

ROIsegNet is evaluated thoroughly in terms of segmentation performance against multiple evaluation metrics on the DMR-IR data set [41] in our experiments. The framework achieved an accuracy of up to 96.8%, IoU up to 93.8%, precision up to 96.2% Dice Loss at minimum or 0.034. ROIsegNet achieves segmentation accuracy enhancement consistently by 1–7% across all important performance metrics compared to traditional deep learning architectures, while being more generalisable and robust across the modalities condition. These results validate the suggested framework for robust and faithful segmentation of thermographic ROIs.

One of the major contributions of this work over any other study is the coupling of projections using ISBROI with anatomy-aware refinement that leads to a decrease of missed false-positive regions and increase in boundary accuracy. Combination of deep learning with domain-specific constraints is thus shown to result in segmentation results that are more consistent as well as clinically interpretable.

The results as a whole validate that the proposed ROIsegNet can be used as a reliable and efficient automated approach to extracting ROI of a breast, and hence be an asset for a preprocessing step in a breast cancer screening system based on computer aided thermographic analysis using IR image processing and classification techniques.

### **6.2 Future Work**

While the proposed framework is performing well in the intended tasks several future directions can be taken to further improve their applicability and effect. In the first instance, future work will involve validating

ROIsegNet on larger and more generalisable thermographic datasets collected across centres of multiple clinical settings, which can better reflect the imaging conditions and patient populations experienced in clinical practice. Second, the present study is up to two-class segmentation of normal and abnormal regions, but the framework can be extended to a multi-class classification for detecting benign and malignant, for a more complete diagnostic support in future work. Third, the inference complexity of ROIsegNet can be reduced even further via model compression, pruning or knowledge distillation methods with a view to real-time running in mobile or embedded systems with cheap resources.

Moreover, when thermographic data is combined with other imaging methods, such as ultrasound or mammography, then they can result in enhanced diagnosis. The fusion of multi-modal features could be helpful to the model to capture complementary information sources [39]. Other directions in future directions may involve new learning paradigms such as self-supervision to alleviate the use of labelled data, domain adaptation to alleviate between-domain differences at the dataset scale and transfer learning to facilitate cross-modality use. This will give substantial gains in the scalability and adaptability of the framework in application in clinical practice.

The second step entails clinical validation and practical implementation of ROIsegNet in existing healthcare workflows. It will have to work with clinicians to determine its usefulness as a decision support tool in early breast cancer detection. Overall, the current work has shown that thermographic analysis is a multifaceted procedure that ranks the correct and anatomy aware ROI segmentation as a gold-standard procedure, and ROIsegNet offers a safe, generalisable and transferrable to clinical system. This is a good indication of further validation and optimization to play a specific role in non-invasive breast cancer detection and supplementing AI-directed medical diagnostics.

## References

1. R. Karthiga and K. Narasimhan; (2021). Medical imaging technique using curvelet transform and machine learning for the automated diagnosis of breast cancer from thermal image . *Pattern Analysis and Applications*. <http://doi:10.1007/s10044-021-00963-3>
2. Samir S. Yadav and Shivajirao M. Jadhav. (2020). Thermal infrared imaging based breast cancer diagnosis using machine learning techniques. *Springer*. 81, pp.1-19. <https://doi.org/10.1007/s11042-020-09600-3>
3. Raquel Sánchez-Cauce; Jorge Pérez-Martín and Manuel Luque; (2021). Multi-input convolutional neural network for breast cancer detection using thermal images and clinical data . *Computer Methods and Programs in Biomedicine*. <http://doi:10.1016/j.cmpb.2021.106045>
4. Mariana Macedo; Maira Santana; Wellington P. dos Santos; Ronaldo Menezes and Carmelo Bastos-Filho; (2021). Breast cancer diagnosis using thermal image analysis: A data-driven approach based on swarm intelligence and supervised learning for optimized feature selection . *Applied Soft Computing*. <http://doi:10.1016/j.asoc.2021.107533>
5. Barsha Abhisheka, Saroj Kumar Biswas and Biswajit Purkayastha. (2023). A comprehensive review on breast cancer detection, classification and segmentation using deep learning. *Springer*. 30, pp.1-30. <https://doi.org/10.1007/s11831-023-09968-z>
6. Dennies Tsietso, Abid Yahya, Ravi Samikannu, Muhammad Usman Tariq, Muhammad Babar, Basit Qureshi And Anis Koubaa. (2023). Multi-Input Deep Learning Approach for Breast Cancer Screening Using Thermal Infrared Imaging and Clinical Data. *IEEE*. 11, pp.52101 - 52116. <http://DOI:10.1109/ACCESS.2023.3280422>
7. Venkatesan Rajinikanth; Seifedine Kadry; David Taniar; Robertas Damasevicius and Hafiz Tayyab Rauf; (2021). Breast-Cancer Detection using Thermal Images with Marine-Predators-Algorithm Selected Features. 2021 Seventh International conference on Bio Signals, Images, and Instrumentation (ICBSII). <http://doi:10.1109/icbsii51839.2021.9445166>
8. Houssein, Essam H.; Emam, Marwa M.; Ali, Abdelmgeid A. and Suganthan, PonnuthuraiNagaratnam (2020). Deep and machine learning techniques for medical imaging-based breast cancer: A comprehensive review. *Expert Systems with Applications*, 114161-. <http://doi:10.1016/j.eswa.2020.114161>
9. Aigerim Mashekova, Yong Zhao, Eddie Y.K. Ng, Vasilios Zarikas, Sai Cheong Fok and Olzhas Mukhmetov. (2022). Early detection of the breast cancer using infrared technology – A comprehensive review. *Elsevier*. 27, pp.1-18. <https://doi.org/10.1016/j.tsep.2021.101142>

10. Resmini, R., Faria da Silva, L., Medeiros, P. R. T., Araujo, A. S., Muchaluat-Saade, D. C., & Conci, A. (2021). *A hybrid methodology for breast screening and cancer diagnosis using thermography*. *Computers in Biology and Medicine*, 135, 104553. <http://doi:10.1016/j.compbiomed.2021.104>
11. Houssein, E. H., Emam, M. M., & Ali, A. A. (2021). An efficient multilevel thresholding segmentation method for thermography breast cancer imaging based on improved chimp optimization algorithm. *Expert Systems with Applications*, 185, 115651. <http://doi:10.1016/j.eswa.2021.115651>
12. Lakshman K; Siddharth B. Dabhade; Y. S. Rode; Karan Dabhade; S. Deshmukh and Ranjan Maheshwari; (2021). Identification of Breast Cancer from Thermal Imaging using SVM and Random Forest Method. 2021 5th International Conference on Trends in Electronics and Informatics (ICOEI). <http://doi:10.1109/icoei51242.2021.9452809>
13. Zeiser, F. A., da Costa, C. A., Ramos, G. de O., Bohn, H. C., Santos, I., & Roehe, A. V. (2021). *DeepBatch: A hybrid deep learning model for interpretable diagnosis of breast cancer in whole-slide images*. *Expert Systems with Applications*, 185, 115586. <http://doi:10.1016/j.eswa.2021.115586>
14. Zahra Rezaei; (2021). A review on image-based approaches for breast cancer detection, segmentation, and classification. *Expert Systems with Applications*. <http://doi:10.1016/j.eswa.2021.115204>
15. Liu, Z., Ni, S., Yang, C., Sun, W., Huang, D., Su, H., ... Qin, N. (2021). Axillary lymph node metastasis prediction by contrast-enhanced computed tomography images for breast cancer patients based on deep learning. *Computers in Biology and Medicine*, 136, 104715. <http://doi:10.1016/j.compbiomed.2021.104715>
16. Krithiga, R. and Geetha, P. (2020). Breast Cancer Detection, Segmentation and Classification on Histopathology Images Analysis: A Systematic Review. *Archives of Computational Methods in Engineering*. <http://doi:10.1007/s11831-020-09470-w>
17. Sharma, R., Sharma, J. B., Maheshwari, R., & Baleanu, D. (2021). Early anomaly prediction in breast thermogram by hybrid model consisting of superpixel segmentation, sparse feature descriptors and extreme learning machine classifier. *Biomedical Signal Processing and Control*, 70, 103011. <http://doi:10.1016/j.bspc.2021.103011>
18. Jun Bai; Russell Posner; Tianyu Wang; Clifford Yang and Sheida Nabavi; (2021). Applying deep learning in digital breast tomosynthesis for automatic breast cancer detection: A review . *Medical Image Analysis*. <http://doi:10.1016/j.media.2021.102049>
19. Bardia Yousefi; Hossein Memarzadeh Sharifipour and Xavier P. V. Maldague; (2021). A Diagnostic Biomarker for Breast Cancer Screening via Hilbert Embedded Deep Low-Rank Matrix Approximation . *IEEE Transactions on Instrumentation and Measurement*. <http://doi:10.1109/tim.2021.3085956>
20. Chen Chen; Yong Wang; Jianwei Niu; Xuefeng Liu; Qingfeng Li and Xuanton Gong; (2021). Domain Knowledge Powered Deep Learning for Breast Cancer Diagnosis Based on Contrast-Enhanced Ultrasound Videos . *IEEE Transactions on Medical Imaging*. <http://doi:10.1109/tmi.2021.3078370>
21. [Tariq, Mehreen; Iqbal, Sajid; Ayesha, Hareem; Abbas, Ishaq; Ahmad, Khawaja Tehseen and Niazi, Muhammad Farooq Khan (2020). Medical Image based Breast Cancer Diagnosis: State of the Art and Future Directions. *Expert Systems with Applications*, 114095-. <http://doi:10.1016/j.eswa.2020.114095>
22. Nienke Bakx, Dorien Rijkaart, Maurice van der Sangen, Jacqueline Theuws , Peter-Paul van der Toorn, An-Sofie Verrijssen, Jorien van der Leer, Joline Mutsaers, Th´er`ese van Nunen, Marjon Reinders, Inge Schuengel, Julia Smits, Els Hagelaar, Dave van Gruijthuijsen, Johanna Bluemink and Coen Hurkmans. (2023). Clinical evaluation of a deep learning segmentation model including manual adjustments afterwards for locally advanced breast cancer. *Elsevier*. 26, pp.1-6. <https://doi.org/10.1016/j.tipsro.2023.100211>
23. Rahul Kumar Yadav, Pardeep Singh and Poonam Kashtriya. (2023). Diagnosis of Breast Cancer using Machine Learning Techniques -A Survey. *Elsevier*. 218, pp.1434-1443. <https://doi.org/10.1016/j.procs.2023.01.122>
24. Chang Li and Xi Lu; (2021). Computer-Aided Detection Breast Cancer in Whole Slide Image . 2021 International Conference on Computer, Control and Robotics (ICCCR). <http://doi:10.1109/icccr49711.2021.9349391>
25. Seifedine Kadry; Robertas Damasevicius; David Taniar; Venkatesan Rajinikanth and Isah A. Lawal; (2021). Extraction of Tumour in Breast MRI using Joint Thresholding and Segmentation – A Study . 2021 Seventh International conference on Bio Signals, Images, and Instrumentation (ICBSII). <http://doi:10.1109/icbsii51839.2021.9445152>
26. Yun Peng, Wei Tang and Xiaoyu Peng. (2023). The study of ultrasonography based on deep learning in breast cancer. *Elsevier*. 16(4), pp.1-7. <https://doi.org/10.1016/j.jrras.2023.100679>
27. Sruthi Krishna and Betsy George; (2021). An affordable solution for the recognition of abnormality in breast thermogram . *Multimedia Tools and Applications*. <http://doi:10.1007/s11042-021-11082-w>

28. Jessiane M. S. Pereira; Maíra A. Santana; Juliana C. Gomes; Valter Augusto de Freitas Barbosa; Mêuser Jorge Silva Valença; Sidney Marlon Lopes de Lima and Wellington Pinheiro dos Santos; (2021). Feature selection based on dialectics to support breast cancer diagnosis using thermographic images . Research on Biomedical Engineering. <http://doi:10.1007/s42600-021-00158-z>
29. Meenalochini, G. and Ramkumar, S. (2020). Survey of machine learning algorithms for breast cancer detection using mammogram images. Materials Today: Proceedings, S2214785320364257-. <http://doi:10.1016/j.matpr.2020.08.543>
30. Mishra, S., Prakash, A., Roy, S. K., Sharan, P., & Mathur, N. (2020). Breast Cancer Detection using Thermal Images and Deep Learning. 2020 7th International Conference on Computing for Sustainable Global Development (INDIACom). doi:10.23919/indiacom49435.2020.9083722
31. Ibrahim, Abdelhameed; Mohammed, Shaimaa; Ali, Hesham Arafat and Hussein, Sherif E. (2020). Breast Cancer Segmentation from Thermal Images Based on Chaotic Salp Swarm Algorithm. IEEE Access, 1–1. <http://doi:10.1109/ACCESS.2020.3007336>
32. Kakileti, Siva Teja; Manjunath, Geetha and Madhu, Himanshu J. (2019). 41st Annual International Conference of the IEEE Engineering in Medicine and Biology Society (EMBC) - Cascaded CNN for View Independent Breast Segmentation in Thermal Images. 6294–6297. <http://doi:10.1109/embc.2019.8856628>
33. Husaini, Mohammed Abdulla Salim Al; Habaebi, Mohamed Hadi; Hameed, Shihab A.; Islam, Md. Rafiqul and Gunawan, Teddy Surya (2020). A Systematic Review of Breast Cancer Detection Using Thermography and Neural Networks. IEEE Access, 8, 208922–208937. <http://doi:10.1109/ACCESS.2020.3038817>
34. Raghavendra, U; Gudigar, Anjan; Rao, Tejaswi N; Ciaccio, Edward J; Ng, E.Y.K. and Rajendra Acharya, U. (2019). Computer aided diagnosis for the identification of breast cancer using thermogram images: A comprehensive review. Infrared Physics & Technology, 103041–. <http://doi:10.1016/j.infrared.2019.103041>
35. Farooq, Muhammad Ali and Corcoran, Peter (2020). 31st Irish Signals and Systems Conference (ISSC) - Infrared Imaging for Human Thermography and Breast Tumor Classification using Thermal Images. 1–6. <http://doi:10.1109/ISSC49989.2020.9180164>
36. Singh, Deepika and Singh, Ashutosh Kumar (2020). Role of image thermography in early breast cancer detection- Past, present and future. Computer Methods and Programs in Biomedicine, 183, 105074–. <http://doi:10.1016/j.cmpb.2019.105074>
37. Kakileti, Siva Teja; Madhu, Himanshu J.; Manjunath, Geetha; Wee, Leonard; Dekker, Andre and Sampangi, Sudhakar (2020). Personalized risk prediction for breast cancer pre-screening using artificial intelligence and thermal radiomics. Artificial Intelligence in Medicine, 105, 101854–. <http://doi:10.1016/j.artmed.2020.101854>
38. Sánchez-Ruiz, Daniel; Olmos-Pineda, Ivan and Olvera-López, J. Arturo (2020). Automatic region of interest segmentation for breast thermogram image classification. Pattern Recognition Letters, 135, 72–81. <http://doi:10.1016/j.patrec.2020.03.025>
39. Mahmood, Tariq; Li, Jianqiang; Pei, Yan; Akhtar, Faheem; Imran, Azhar and Rehman, Khalil ur (2020). A Brief Survey on Breast Cancer Diagnostic with Deep Learning Schemes Using Multi-Image Modalities. IEEE Access, 1–1. <http://doi:10.1109/ACCESS.2020.3021343>
40. P, Gomathi; C, Muniraj and PS, Periasamy (2020). Breast Thermography Based Unsupervised Anisotropic-Feature Transformation Method For Automatic Breast Cancer Detection. Microprocessors and Microsystems, 103137–. <http://doi:10.1016/j.micpro.2020.103137>
41. DMR - Database for Mastology Research. Retrieved from <http://visual.ic.uff.br/dmi/>
42. Y. LeCun, B. Boser, J. S. Denker, D. Henderson, R. E. Howard, W. Hubbard, and L. D. Jackel. Backpropagation applied to handwritten zip code recognition. Neural computation, 1(4):541–551, 1989.
43. P. Sermanet, D. Eigen, X. Zhang, M. Mathieu, R. Fergus, and Y. LeCun. Overfeat: Integrated recognition, localization and detection using convolutional networks. arXiv:1312.6229, 2013.
44. A. Krizhevsky, I. Sutskever, and G. E. Hinton. Imagenet classification with deep convolutional neural networks. In NIPS, 2012.
45. Li, Mingfeng. (2024). Comprehensive Review of Backpropagation Neural Networks. Academic Journal of Science and Technology. 9. 150-154. 10.54097/51y16r47.
46. Anusooya, G., Bharathiraja, S., Mahdal, M., Satharajasekaran, K., & Elangovan, M. (2023). Self-Supervised Wavelet-Based Attention Network for Semantic Segmentation of MRI Brain Tumor. *Sensors*, 23(5), 2719. <https://doi.org/10.3390/s23052719>
47. A. Giusti, D. C. Cireşan, J. Masci, L. M. Gambardella and J. Schmidhuber, "Fast image scanning with deep max-pooling convolutional neural networks," 2013 IEEE International Conference on Image Processing, Melbourne, VIC, Australia, 2013, pp. 4034-4038, doi: 10.1109/ICIP.2013.6738831.

48. L.-C.Chen,G.Papandreou,I.Kokkinos,K.Murphy,andA.L. Yuille. Deeplab: Semantic image segmentation with deep convolutional nets, atrous convolution, and fully connected crfs. arXiv:1606.00915, 2016.
49. Brandt, A. (1977). Multi-level adaptive solutions to boundary-value problems. *Mathematics of Computation*, 31(138), 333–390. <https://doi.org/10.1090/S0025-5718-1977-0431719-X>
50. Liu, X., Li, X., Chen, H., & Heng, P. A. (2020). Deep learning optimization landscape and training dynamics: A survey. *IEEE Transactions on Pattern Analysis and Machine Intelligence*. <https://doi.org/10.1109/TPAMI.2020.3032376>
51. Lin, T.-Y., Dollár, P., Girshick, R., He, K., Hariharan, B., & Belongie, S. (2017). Feature pyramid networks for object detection. *CVPR 2017*. <https://doi.org/10.1109/CVPR.2017.106>
52. Yuan, Y., et al. (2020). Object-Contextual Representations for Semantic Segmentation. *ECCV 2020*. [https://doi.org/10.1007/978-3-030-58529-7\\_40](https://doi.org/10.1007/978-3-030-58529-7_40)
53. W. Liu, A. Rabinovich, and A. C. Berg. Parsenet: Looking wider to see better. arXiv:1506.04579, 2015.
54. S. Ioffe and C. Szegedy. Batch normalization: Accelerating deep network training by reducing internal covariate shift. arXiv:1502.03167, 2015.
55. Chen, L.C., Papandreou, G., Schroff, F., Adam, H.: Rethinking atrous convolution for semantic image segmentation. arXiv:1706.05587 (2017)
56. Ronneberger, O., Fischer, P., Brox, T.: U-net: Convolutional networks for biomedical image segmentation. In: MICCAI. (2015).
57. T M Sathish Kumar, & Shaik Sadulla. (2026). Smart Cities, Equal Futures: Integrating Gender Perspectives into Sustainable Urban Innovation. *Journal of Women, Innovation, and Technological Empowerment*, 2(1), 1-7. <https://aasrresearch.com/index.php/jwite/article/view/354>
58. Madhanraj, & Sumit Ramswami Punam. (2026). Mechanistic Simulation of Microbial Transport and Diffusion Processes for Planetary Contamination Control Using Cellular Automata. *Advances in Mechanical Engineering and Applications*, 2(1), 10-17. <https://aasrresearch.com/index.php/amea/article/view/151>
59. K. Geetha, &M.Karpagam. (2026). Integrating Traditional Yogic Practices with Modern Exercise Science for Sustainable Wellness in Aging Populations. *Journal of Yoga, Sports, and Health Sciences*, 24-30. <https://aasrresearch.com/index.php/ayshs/article/view/406>
60. Vimalkumar T. (2025). Adaptive Synchronization of Nonlinear Neural Oscillator Networks Under Time-Delay Perturbations. *Applied Nonlinearity in Science and Technology*, 1-5.